as RuBisCO, quantification of Mn^{2+}-activated RuBisCO in chloroplasts will be important.

REFERENCES

Adam, W., Cuerto, O., & Rebollo, H. (1982) *Angew. Chem., Int. Ed. Engl. 21*, 75.
Berhow, M. A., Saluja, A., & McFadden, B. A. (1982) *Plant. Sci. Lett. 27*, 51-57.
Christeller, J. T. (1981) *Biochem. J. 193*, 839-844.
Deneke, C. F., & Krinsky, N. I. (1976) *J. Am. Chem. Soc. 98*, 3041-3042.
Deneke, C. F., & Krinsky, N. I. (1977) *Photochem. Photobiol. 25*, 299-304.
Foote, C. S., Fujimoto, T. T., & Chang, Y. C. (1972) *Tetrahedron Lett.* 45-48.
Horrocks, D. L. (1974) in *Applications of Liquid Scintillation Counting*, p 81, Academic Press, New York and London.
Jordan, D. B., & Ogren, W. L. (1983) *Arch. Biochem. Biophys. 227*, 425-433.
Kajiwara, T., & Kearns, D. (1973) *J. Am. Chem. Soc. 95*, 5886-5890.
Khan, A. U., & Kasha, M. (1970) *J. Am. Chem. Soc. 92*, 3293-3300.
Kreckl, W., Kexel, H., Melzer, E., & Schmidt, H. L. (1989) *J. Biol. Chem. 264*, 10982-10986.
Laing, W. A., Ogren, W. L., & Hageman, R. H. (1974) *Plant. Physiol. 54*, 678-685.
Lorimer, G. H. (1981) *Annu. Rev. Plant Physiol. 32*, 349-383.
Lorimer, G. H., & Andrews, T. J. (1973) *Nature 243*, 359-360.
McFadden, B. A. (1973) *Bacteriol. Rev. 37*, 289-319.
McFadden, B. A., Torres-Ruiz, J. A., Daniell, H., & Sarojini, G. (1986) *Philos. Trans. R. Soc. London, B 313*, 347-358.
Miziorko, H. M., & Lorimer, G. H. (1983) *Annu. Rev. Biochem. 52*, 507-535.
Ogryzlo, E. A., & Tang, C. W. (1970) *J. Am. Chem. Soc. 92*, 5034-5036.
Pierce, J., Tolbert, N. E., & Barker, R. (1980) *Biochemistry 19*, 934-942.
Spikes, J. D., & Swartz, H. M. (1978) *Photochem. Photobiol. 28*, 921-933.
Tabita, F. R., & McFadden, B. A. (1974) *J. Biol. Chem. 249*, 3459-3464.
Wildner, G. F., & Henkel, J. (1979) *Planta 146*, 223-228.
Wilson, T., & Hastings, J. W. (1970) *Photophysiology 5*, 49-95.

A Delay in Membrane Fusion: Lag Times Observed by Fluorescence Microscopy of Individual Fusion Events Induced by an Electric Field Pulse

Dimiter S. Dimitrov[‡] and Arthur E. Sowers*[,§]

Cell Biology, Holland Laboratory, American Red Cross, 15601 Crabbs Branch Way, Rockville, Maryland 20855

Received January 18, 1990; Revised Manuscript Received May 29, 1990

ABSTRACT: Low light level video microscopy of the fusion of DiI- (1,1′-dihexadecyl-3,3,3′,3′-tetramethylindocarbocyanine perchlorate) labeled rabbit erythrocyte ghosts with unlabeled rabbit erythrocyte ghosts, held in stable apposition by dielectrophoresis in sodium phosphate buffers, showed reproducible time intervals (delays) between the application of a single fusogenic electric pulse and the earliest detection of fluorescence in the unlabeled adjacent membranes. The delay increased over the range 0.3–4 s with a decrease in (i) the electric field strength of the fusion-inducing pulse from 1000 to 250 V/mm, (ii) the decay half-time of the fusogenic pulse in the range 1.8–0.073 ms, and (iii) the dielectrophoretic force which brings the membranes into close apposition. A change in the buffer viscosity from 1.8 to 10 mP·s caused the delay to increase from 0.36 to 3.7 s (in glycerol solutions) or to 5.2 s (in sucrose solutions). The delay decreased 2–3 times with an increase in temperature from 21 to 37 °C. It did not differ significantly for "white" ghosts [0.013 mM hemoglobin (Hb)] or "red" ghosts (0.15 mM Hb) or buffer strength over the range 5–60 mM (sodium phosphate, pH 8.5). The calculated activation energy, 17 kcal/mol, does not depend on the field strength. The yield of fused cells was high when the delay was short. The delay in electrofusion resembles the delays in pH-dependent fusion of vesicular stomatitis viruses with erythrocyte ghosts [Clague, M. J., Schoch, C., Zech, L., & Blumenthal, R. (1990) *Biochemistry 29*, 1303–1308] and of fibroblasts expressing influenza hemagglutinin and red blood cells [Morris, S. J., Sarkar, D. P., White, J. M., & Blumenthal, R. (1989) *J. Biol. Chem. 264*, 3972–3978]. The delay reflects the lifetime of a long-lived intermediate state in fusion. It may be partly due to the time of mutual approach of membranes needed to reach molecular contact and/or the time of relatively slow molecular rearrangements leading to formation of intermembrane connections.

Membrane fusion is a process which converts two membranes into one, thereby permitting membrane mixing and the removal of the membrane barrier or contents mixing. One proposal, for example, suggests that cell fusion involves six possible stages (Rand & Parsegian, 1986): (i) stable membrane apposition, (ii) triggering of fusion, (iii) contact, (iv) focused destabilization, (v) membrane coalescence, and (vi) restabilization. The time interval between the triggering and the membrane coalescence (the actual fusion event) is usually considered to be very short. Time-resolved freeze–fracture electron microscopy suggests that during neurotransmitter release this time (delay in fusion) is less than 5 ms (Heuser et al., 1979). This is the same order of magnitude of the time for exocytosis in other systems (Plattner, 1989). Studies of

[‡] Permanent address: Central Laboratory of Biophysics, Bulgarian Academy of Sciences, Sofia 1113, Bulgaria.
[§] Supported by ONR Grant N00014-89-J-1715.

0006-2960/90/0429-8337$02.50/0

vesicle–vesicle fusions (Hoekstra et al., 1985; Duzgunes et al., 1987; Meers et al., 1988; Rupert et al., 1988; Siegel et al., 1989) and vesicle–lipid bilayer fusions (Cohen et al., 1984, 1989; Niles & Cohen, 1987; Woodbury & Hall, 1988a,b) did not indicate any delays within the time resolution of their methods, which is of the order of seconds. For planar–planar bilayer fusions (Chernomordik et al., 1987) the lifetimes of the events leading to fusion ("waiting time" for fusion) have been measured to be in the range of seconds to minutes. Delays in viral envelope protein induced fusion events also can take up to 10 s (Morris et al., 1989; Clague et al., 1990) or more (Hoekstra et al., 1989; Spruce et al., 1989) for completion. Interestingly, there was no delay in the fusion of Sendai viruses with liposomes (the time resolution of the method was of the order of seconds) [see Figure 7 in Hoekstra & Wilschut (1989)], while at similar conditions delays of the order of minutes were measured for fusion of Sendai viruses with erythrocyte ghosts (Hoekstra et al., 1989). Fluorescence spectroscopy studies, based on water-soluble probes, did not show any measurable delays in erythrocyte electrofusion (Stenger & Hui, 1989). However, the lack of delays in electrofusion, measured by water-soluble probes, has now been shown to be due to the fast electroosmotic exchange of the fluorescence probe through the pores before the membrane fusion takes place (Sowers, 1988; Dimitrov & Sowers, 1990). Time-resolved X-ray diffraction showed a half-time of about 3 min for fusion of hexagonal and lamellar lipid structures resulting in a lamellar phase (Laggner, 1988). It has been theoretically estimated that the lifetime of intermediates between lamellar and inverted hexagonal lipid phases, which can play a role in fusion, may be in the millisecond time range scale (Siegel, 1984, 1986).

Measuring the lifetime of intermediates in fusion is difficult for several reasons. First, creating the chemical changes in the suspension medium which lead to fusogenic conditions will require a minimum time for complete mixing. Stopped-flow kinetics chambers are among the fastest mixing systems known and have mixing times in the 50-ms range (Clague et al., 1990). Second, any fusion assay will require a minimum time after fusion for the fusion product to become detectable. For spectrofluorometric assays this time can be as short as 50 ms but is typically in the range of seconds. Third, fluorescence intensities may be so low that data on fusion processes must be obtained by use of large populations of fusion events.

Early studies of fusion in individual pairs of membranes (Zimmermann, 1982) could not determine the delays in fusion events because what was detected after fusion was the rounding-up process and not fusion, per se. Recent studies of virus–cell fusions show that single fusion events are detectable (Sarkar et al., 1989; Georgiou et al., 1989) and suggest that the events leading to fusion may have lifetimes long enough to be measured. In the present study a new approach is used to study the lifetimes of events leading to fusion of individual membranes. A strong exponentially decaying electric field pulse is used as a nonchemical fusogen. This has the advantages that (i) all fusion processes are initiated within the rise time of the pulse (<1 μs), (ii) the fusogen is essentially absent from the system 10–12 ms after the pulse was applied, and (iii) the high yields of fusion which are possible with this fusogen make practicable the use of low light level video microscopy to not only detect individual fusion events but also measure several fusion-related parameters. In addition, the present study utilizes alternating current induced dielectrophoresis (Pohl, 1978) to bring membranes into contact (Dimitrov et al., 1990). This method of inducing close membrane–membrane contact has the advantages that it is (i) mild, (ii) reversible, and (iii) nonchemical. This permits both the conditions for inducing membrane–membrane apposition and those for the application of fusogen to be separated from the chemistry of the membrane suspension. Analysis of our approach indicates that merging of the membranes can be determined within 17 ms after the completion of the fusion event. Our results show that membrane coalescence can take place, depending on conditions, up to 5 s and longer after the fusion process is triggered. These lag times (delays) decreased drastically in proportion to (i) the fusogen pulse strength, (ii) the temperature, (iii) the inverse of the intermembrane separation, and (iv) the decrease of the viscosity of the aqueous medium.

Materials and Methods

Cells and Media. Erythrocyte ghosts were obtained from rabbits by hypotonic lysis (Dodge et al., 1963), washed, and stored in 20 mM sodium phosphate buffer (NaP_i) (pH 8.5, 4 °C) (Sowers, 1989a,b). Briefly, 2 mL of packed red blood cells were added to 40 mL of 5 mM sodium phosphate buffer and kept on ice for 20 min. This suspension was spun for 10 min at 9000*g* to obtain a pellet of red ghosts. The red ghosts were then washed in 20 mM buffer. The white ghosts were obtained by adding 5 mM phosphate buffer to the pellet of red ghosts and keeping them for 2 h in ice. Then they were centrifuged at 9000*g* for 10 min and washed with 20 mM phosphate buffer.

The hemoglobin concentration in the ghosts was determined spectrophotometrically with Triton X-100 as a detergent to dissolve the membranes. Red and white ghosts contained 2.7% (0.15 mM) and 0.23% (0.013 M), respectively, of the total hemoglobin concentration in the intact red blood cell. Red ghosts were used in all experiments unless otherwise specified or where comparisons were made between red and white ghosts. The membranes were labeled with the fluorescent dye DiI (1,1′-dihexadecyl-3,3,3′,3′-tetramethylindocarbocyanine perchlorate) (Molecular Probes) as previously described (Sowers, 1986). Briefly, 0.01 mL of stock solution of DiI (3.5 mg/mL in absolute ethanol) was added while 1 mL of the buffer containing 0.1 mL of pelleted ghosts was being vortexed. After standing for 1 min, the excess DiI was removed by washing with 20 mM NaP_i buffer at 8000*g* for 10 min at 0–4 °C. The labeled ghosts were stored as a pellet in a refrigerator. Labeled ghosts were mixed with unlabeled at a ratio of 1:10. The cell concentration in the suspension used for the experiments corresponded to an average distance between the ghost surfaces of the order of their radii. The ionic strength of the medium was varied by changing the buffer concentration. We used 5, 20, and 60 mM sodium phosphate solution (pH 8.5). The viscosity of the medium was adjusted by adding glycerol or sucrose. The viscosity values were from a handbook (Weast, 1989). Most of the data came from experiments that utilized ghosts from the same rabbit (age: 6 months). Only the experiments on temperature dependence were carried out with ghosts from this and two additional rabbits (age: 6 and 18 months). The experiments were performed at 21 ± 1, 24 ± 0.5, 28 ± 1, and 37 ± 1 °C.

Chamber and Electric Field. All observations were made with the rectangular chamber described in Sowers (1984). The AC sine wave field had a frequency of 60 Hz and a field strength (E_{AC}), which was varied from 4 to 32 V/mm (from 8 to 64 V applied across a 2-mm chamber length) (voltages given as root mean square). The DC pulse strength (E) was varied from 0.25 to 1 kV/mm. The pulse decay half-time, which is a measure of the pulse duration, was varied from

0.073 to 1.8 ms. A storage screen oscilloscope was used to monitor both the strength and duration of the fusogenic pulse.

Fluorescence Video Microscopy. Images were viewed by use of a Zeiss Model 14 microscope. They were recorded on video tape in real time by a Zeiss three-stage low light level Venus camera for subsequent single-frame playback and analysis. A Panasonic (Secaucus, NJ) NV-9300A and Colorado Video (Boulder, CO) Model 499 video multimemory were used to examine single frames of video sequences. A FORA (West Newton, MA) Model VTG-22 video timer operated in the stopwatch mode placed an alphanumeric field with date and time information with ±0.01 s frame-to-frame accuracy onto each recorded video frame. To determine exactly when the pulse was applied, a sample of the pulse was used to electronically shift the location of the alphanumerics to a new location about 1 cm higher on the monitor screen. Although the video scans were not synchronized with the pulse, this system allows resolution in time with respect to location of the pulse to be equal to or less than 17 ms. The magnification was determined with a Lafayete objective micrometer and fluorescent calibration spheres (Epics, Hialeah, FL). The fluorescence at any selected pixel was measured by a Colorado Video (Boulder, CO) Model 321 analyzer. The overall system contrast transfer function was determined to be within ±10% of linearity as a function of specimen location in the viewing field by use of cytometer fluorescent calibration spheres (Epics, Hialeah, FL).

Protocols and Data Processing. The chambers were filled with a 3-μL ghost suspension. The AC electric field was applied for 10–60 s to induce membranes to come into contact through pearl chain formation. The ghost membranes were examined under phase contrast for shape changes and membrane contact. The experiments were performed only for membranes with spherical shapes, which make contact in the AC field. The optical system was then converted to fluorescence imaging, and a single high-voltage pulse was applied. The fluorescence transfer from the DiI-labeled ghosts to the unlabeled ghosts was recorded until equilibrium redistribution of the dye, indicated by the increase in brightness of the originally unlabeled membrane to the level of that of the originally labeled membrane.

The image records were analyzed by single-frame playback of video sequences (each frame was 1/60 = 16.7 ms). The period of time between the application of the pulse and the earliest appearance of the fluorescence, as detectable during single-frame playback of video sequences (cf. Figure 1), in the unlabeled membrane was defined as the delay, t_d. The moment when the fluorescence intensity increased at contact between the labeled and the originally unlabeled membranes (at point A in Figure 2, inset) 10% above the value before the application of the pulse was taken as the earliest evidence of fusion. A membrane viewed "edge-on" will have a higher concentration of fluorescent dye with respect to the spatial volume it appears to occupy than a membrane viewed broadside. Hence at the earliest moment after fusion, the appearance of fluorescence in the adjacent unlabeled membrane will resemble a set of two "horns" pointing along and coinciding with the membrane plane [see frames 79:29:04 and 79:32:89 in Figure 1 and see Figure 5 in Sowers (1984)].

The time for the visually detectable front of the laterally diffusing fluorescent dye to reach the poles of the ghost membranes, which were farthest from the originally labeled ghost, was defined as the transit time, t_e. The time for the fluorescence intensity at point C in Figure 2, inset, to increase to at least 80% of the fluorescence at point 0 in Figure 2, inset, was taken to be t_u. The background fluorescence was subtracted from the measured fluorescence. The resulting value was divided by the fluorescence in the center of the labeled membrane. These normalized fluorescence intensities were used in the interpretation of the fusion kinetics.

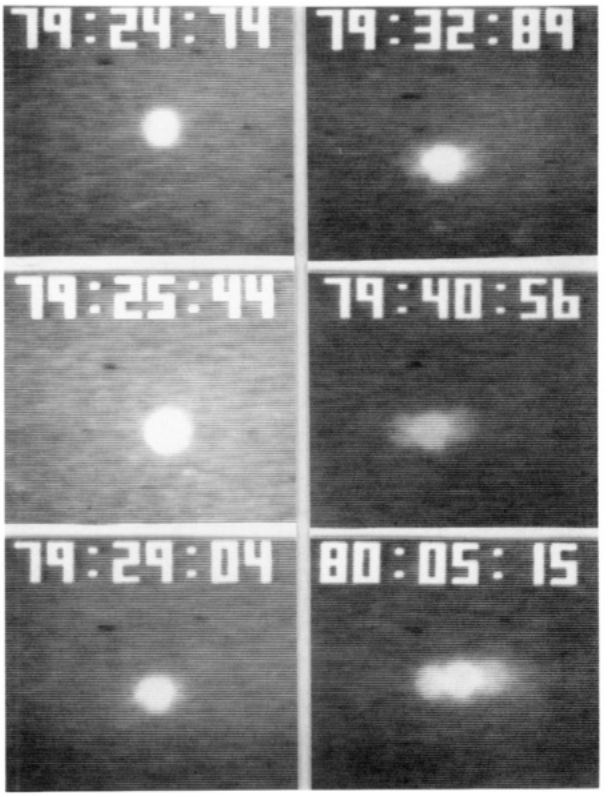

FIGURE 1: Video image sequences showing delay in electrofusion of rabbit erythrocyte ghosts. The delay is indicated by the lag time between application of the pulse and earliest detection of fluorescence transfer to unlabeled membranes. Buffer in medium and cytoplasmic compartments is 20 mM NaP_i (pH 8.5). Alphanumerics: time (min:s:hundredths of s). The electric field is left to right and parallel to the plane of micrographs. The AC field (strength 8 V/mm) is applied at 78:55:00. The cell before the pulse (79:24:74) does not show any indication of fluorescence transfer. The high-voltage electric pulse (strength 0.3 kV/mm, duration 0.9 ms) is applied at 79:25:44. The first appearance of fluorescence as small horns can be seen at 79:29:04. The delay is 3.60 s. The horns increase in length (79:32:89) until reaching the end of the originally unlabeled membranes (79:40:56) and the final state of uniform fluorescence brightness (80:05:15). The width of the alphanumerics is 50 μm. Temperature 24 °C.

Measurements of the recorded images were made on a total of 810 cells. Each experimental point is an average of from 5 to 20 cells.

The fusion yield was calculated from the percentage of all labeled membranes which fuse (Sowers, 1988). It was obtained from counts in the same field of view of both the number of fusion events and the total number of originally labeled membranes (Sowers, 1988). Sample size was always between 80 and 120 cells. The experimental data are the average of three experiments.

Results

Delay in Membrane Electrofusion. Figure 1 shows an example of a video sequence indicating a time interval (delay) between the application of a single fusogenic electric pulse and the appearance of any fluorescence in the originally unlabeled membranes. For this particular case it takes 3.60 s for the earliest detectable appearance of fluorescence in the unlabeled membranes to develop the characteristic horn shape (Figure

Table I: Examples of Variations in Delays, Transit Times, and Equilibrium Times for Six Individual Cells[a]

field strength, E (V/mm)	ghost	delay, t_d (s)	transit time, t_e (s)	equilibrium time, t_u (s)
1000	A	0.31	1.6	3.1
	B	0.36	3.3	13
	C	0.44	6.5	30
300	D	1.6	3.5	12
	E	3.1	8.3	17
	F	5.2	12	23

[a] Buffer strength, 20 mM; pulse decay half-time, 0.9 ms; AC field strength, 8 V/mm; temperature, 21 °C.

1). This was judged by the authors by viewing each frame of the playback of the recorded images. The point where one video frame did not show horns but the subsequent frame did was taken as the time of the earliest appearance of fluorescence in the originally unlabeled membrane. It coincided with an increase of more than 10% in the measured fluorescence intensity at the membrane contact (Figure 2). There was no measurable or visually detectable fluorescence in the originally unlabeled membrane earlier than this time interval. Afterward, the fluorescent dye diffuses laterally in the plane of the membrane until the final state of uniform fluorescence intensity is reached.

Figure 2 shows the measured fluorescence intensity change with time at the corresponding locations indicated in the inset. Some of the fluorescence at the point of membrane contact (A) is from the nearby labeled membrane. The increase in fluorescence begins after time intervals which depend on the locations. These time intervals are proportional to the squares of the separations from the membrane contact. This indicates a diffusional mechanism of the dye transfer after the delay. The dependence is linear with a correlation coefficient higher than 0.99 (data not shown). The diffusion coefficients were calculated from the slopes (equal to $4D$) of these linear dependencies. For example, the diffusion coefficient for the data shown in Figure 2 is 0.55×10^{-8} cm^2/s. For the originally unlabeled membrane on the left in Figure 1, the diffusion coefficient is 0.20×10^{-8} cm^2/s. The spread in the values of the diffusion coefficients is probably due to individual variations between membranes of erythrocyte ghosts.

Our experiments revealed several characteristic features of the delay in the fluorescence transfer: (i) There was always delay in the fluorescence transfer—the time interval, t_d, between the pulse and the earliest indication of fluorescence transfer. (ii) The time intervals to reach the far ends of the membranes, t_e, and the final equilibrium state, t_u, in most cases were correlated with the delays; i.e., there was correlation between the delay and the kinetics of fluorescence increase in the unlabeled ghosts. (iii) The delay increased with a decrease of the electric pulse strength, the pulse duration, the AC electric field strength applied before the pulse to align the membranes, and the temperature; it increased with an increase of the viscosity of the medium. (iv) The delay did not change significantly when the hemoglobin concentration inside the ghosts was varied but did change slightly with the buffer strength. (v) The delay was short when the electrofusion yield was high; the delay changed significantly even when the fusion yield was near saturation (above 80%) and did not change with variation in the pulse strength.

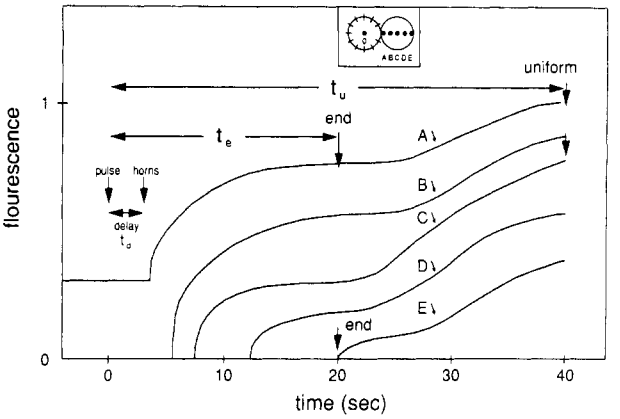

FIGURE 2: Kinetics of fluorescence intensity change for the originally unlabeled membrane on the right side of the originally labeled membrane shown in Figure 1. The space locations of the points of measurement are shown in the inset. The distances from the contact with the labeled membrane area (A) 0 μm (the contact), (B) 1.7 μm, (C) 3.3 μm (the center of the membrane), (D) 5.0 μm, and (E) 6.6 μm (the far right end of the membrane). The membrane diameter is 6.6 μm. The fluorescence is normalized to the fluorescence intensity in the center of the labeled cell (point 0 in the figure in the inset). The fluorescence intensity at the membrane contact (A) is higher than zero before the pulse because of the close proximity of the labeled membrane.

Relationship between Delay, Fluorescent Dye Diffusion Transfer Kinetics, and Fusion Yield. Table I shows examples of delay, transit time, and equilibrium time in six *individual* cells at two pulse strengths: 1000 and 300 V/mm. One can note that ghosts with short delays also have short transit and equilibrium times and vice versa. Small increases in delays correspond to large increases in the transit and equilibrium times. For example, for ghosts A and B (E = 1000 V/mm) the delay increased by 0.36/0.31 = 1.16, while the transit time increased by 3.3/1.6 = 2.1 times and the equilibrium time by 13/3.1 = 4.2 times.

Table II shows the average values of the delays, transit and equilibrium times, and fusion yield for *populations* of membranes (between 8 and 15) for five pulse field strengths. It can be seen that for field strengths between 350 and 1000 V/mm the fusion yield did not change significantly—it was between 85% and 96%. The transit and equilibrium times also did not vary significantly—they were almost the same, noting the relatively large standard deviations. The delay, however, increased by factor of 2.1/0.4 = 5.2 for this pulse strength range. On the other hand, at low voltages (250 and 300 V/mm) the fusion yield changed significantly (from 74% to 20%). However, the delay time and the transit time almost did not change. The equilibrium time increased with a de-

Table II: Average Values and Standard Deviations of Delays, Transit Times, Equilibrium Times, and Fusion Yields for Different Field Strengths of the Fusogenic Pulse[a]

field strength, E (V/mm)	ghosts, N	delay, t_d (s)	transit time, t_e (s)	equilibrium time, t_u (s)	fusion yield (%)
1000	9	0.4 ± 0.1	4 ± 3	16 ± 14	96 ± 3
500	8	1.2 ± 0.2	8 ± 3	17 ± 8	93 ± 5
350	12	2.1 ± 0.4	8 ± 2	19 ± 6	85 ± 10
300	14	3 ± 1	8 ± 3	18 ± 6	74 ± 10
250	15	4 ± 2	10 ± 2	38 ± 10	20 ± 10

[a] Buffer strength, 20 mM; pulse decay half-time, 0.9 ms; AC field strength, 8 V/mm; temperature, 21 °C. N is the number of ghosts in the population.

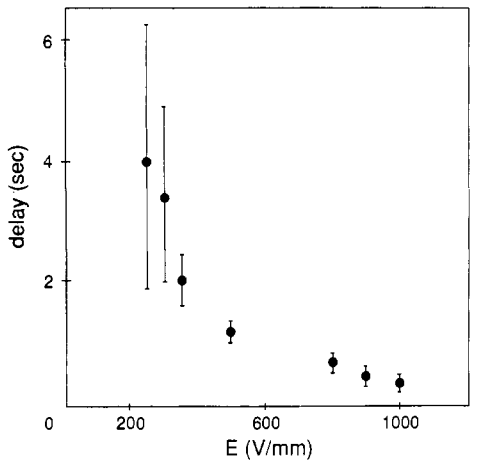

FIGURE 3: Delay in membrane electrofusion as a function of electric field pulse strength. Buffer strength, 20 mM; pulse decay half-time, 0.9 ms; AC field strength, 8 V/mm; temperature, 21 °C.

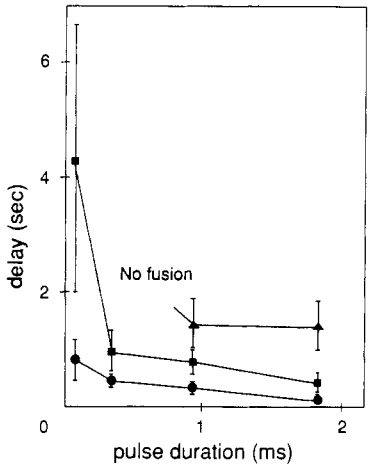

FIGURE 4: Dependence of the delay on the pulse decay half-times for field strengths of 300 (triangles), 500 (squares), and 1000 V/mm (circles). AC field strength, 8 V/mm; buffer strength, 20 mM; temperature, 23 °C. There was no fusion with pulses shorter than 0.35 ms at a field strength of 300 V/mm. For the longest and strongest pulses (pulse duration, 1.8 ms; strength, 1000 V/mm) some of the membranes fragmentated, and some of them formed giant cells; the delay was less than 0.1 s.

crease in the pulse strength from 300 to 250 V/mm, but the standard deviation is large, and this increase may not be so significant.

Pulse Field Strength Dependence. There was a strong decrease in the delay with an increase in the electric pulse strength (Figure 3). The standard deviation in the delay was large only at small pulse strengths (250–300 V/mm). In this field strength range its ratio to the mean value varied between 0.3 and 0.5. The standard deviation in the delay was smaller at higher field strengths. The ratio of the standard deviation to the mean value was in the range of 0.1–0.2 for field strengths between 350 and 1000 V/mm.

Short Pulses Caused Long Delays. The delay decreased with an increase in the pulse decay half-times, which describe the pulse duration (Figure 4). The significant change occurred for pulses with duration below 0.9 ms. There was no fusion for short pulses (<0.5 ms) if the pulse field strength was smaller than 300 V/mm. A pulse with a high field strength (1000 V/mm) and a long pulse decay half-time (1.7 ms) fragmentated the membranes, and about half of them fused and converted to giant cells (diameters of the order of 30 μm and larger). The standard deviation was large only for short and low strength pulses.

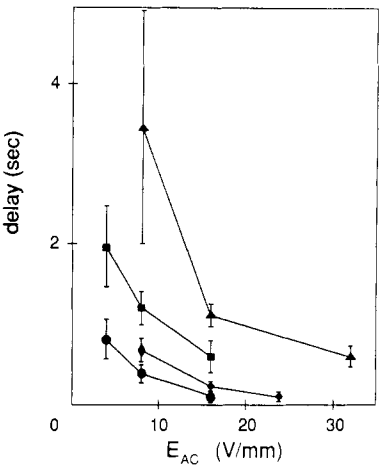

FIGURE 5: Dependence of the delay on the AC field strength for field strengths of 300 (triangles), 500 (squares), 800 (rhomboids), and 1000 V/mm (circles) (pulse duration 0.9 ms). Buffer strength, 20 mM; temperature, 23 °C.

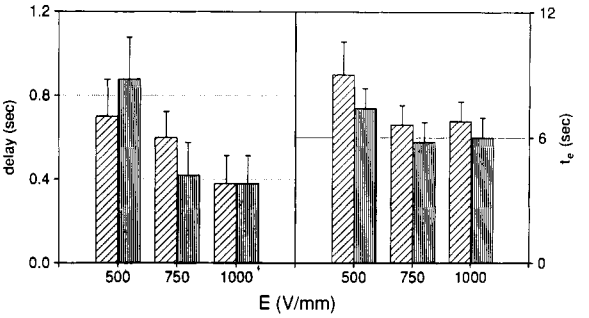

FIGURE 6: Delay and transit time, t_e, in electrofusion of white (0.23% Hb) (the left bar of each pair of bars) and red (2.7% Hb) (the right bar of each pair of bars) ghosts for field strengths of 500, 750, and 1000 V/mm. Buffer strength, 20 mM; pulse decay half-time, 0.9 ms; AC field strength, 8 V/mm; temperature, 21 °C.

AC Field Strength Affected Delays. A decrease in the delay occurred both with an increase of the strength of the AC field, which brings the membranes at close apposition, and with an increase in the pulse strength (range from 300 to 1000 V/mm) (Figure 5). One can note that the major change in the delay occurred for an AC field strength of 16 V/mm. Below this field strength the delay increased significantly. The standard deviation was much larger for low AC and pulse strengths than for high AC and pulse strengths.

Internal Hemoglobin Concentration Did Not Significantly Affect the Delay and the Transit Time. Figure 6 shows the delays and the transit times for internal residual hemoglobin concentrations of 0.013 mM (0.23%) and 0.15 mM (2.7%) at three different field strengths: 500, 750, and 1000 V/mm. The difference between the red (2.7%) and white (0.23%) ghosts was not statistically significant. The standard deviation was almost the same for red and white ghosts.

Delay, Transit, and Equilibrium Times Were Not Significantly Affected by the Buffer Strength. Figure 7 shows that the three characteristic times are shortest at 20 mM, where the fusion yield is maximal. However, the dependence is not statistically significant because there is an overlap of the standard deviations. The standard deviations did not depend significantly on the buffer strength.

Delays Increased with Medium Viscosity. An increase in the viscosity of the medium, adjusted by addition of glycerol or sucrose, led to longer delays (Figure 8). It can be seen that it is almost independent of whether glycerol or sucrose was used. The standard deviation is larger at high viscosities than at low viscosities.

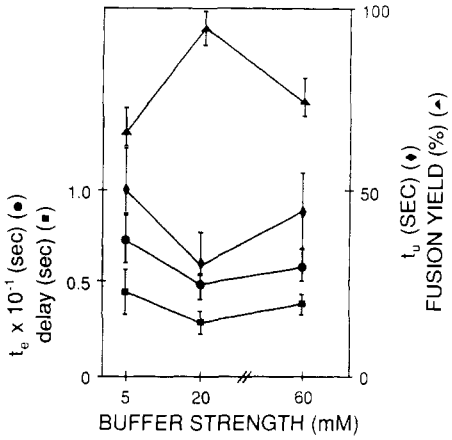

FIGURE 7: Effect of the buffer strength on delay, transit time, t_e, equilibrium time, t_u, and fusion yield. Pulse field strength, 1000 V/mm; duration, 0.9 ms; AC field strength, 8 V/mm; temperature, 23 °C.

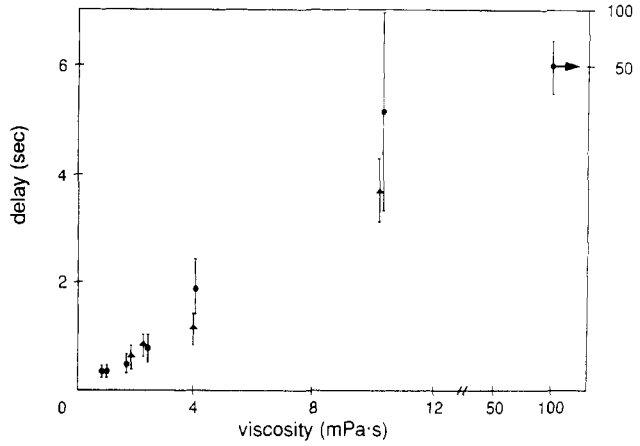

FIGURE 8: Dependence of the delay on medium viscosity. The viscosity was changed by addition of glycerol (circles) or sucrose (triangles). Pulse strength, 1000 V/mm; duration, 0.9 ms; AC field strength, 8 V/mm; buffer strength, 20 mM; temperature, 23 °C.

Temperature Dependence of Delay. The delay decreased with an increase of temperature (Figure 9). The Arrhenius plot (Figure 9B) gives an activation energy of 17 kcal/mol for erythrocyte ghosts from a young rabbit (age: 6 months) and a breakpoint at 28 °C for ghosts from another rabbit (age: 18 months). The diffusion coefficients, calculated from the data (not shown) for the kinetics of the dye transfer, increased 2–3 times with an increase in temperature from 21 to 37 °C. The standard deviations decreased slightly with an increase in temperature.

Discussion

Delays in Membrane Electrofusion. The main new result of this work is the finding of a delay in membrane electrofusion kinetics and that the delay is sensitive to the strength and duration of the fusogen (electric field), the force which brings the membranes at close apposition, and the temperature and viscosity of the medium. That the delay is not due only to diffusion is supported by the following estimate. The first indication of fusion is seen as a characteristic geometric form (horns; see Results). The order of magnitude of the diffusion time to form the horns is $t_D = x^2/4D$, where x is the characteristic distance from the periphery of the membrane–membrane contact to the leading edge of fluorescence (length of the horns), which can be resolved with the microscope (typically 0.3–0.5 μm), and D is the diffusion coefficient of the fluorescent probe [of the order of 10^{-8} cm^2/s (Sowers,

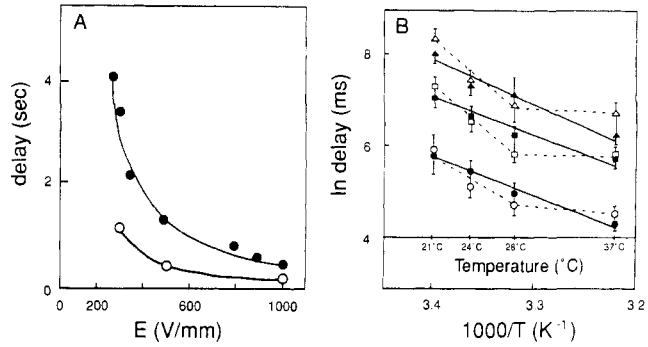

FIGURE 9: Temperature dependence of the delay. (A) Delay as a function of field strength for 22 °C (solid circles) and 37 °C (empty circles). The rabbit is the same as for the data presented in Figure 3, but the experiments were performed on different days. (B) Arrhenius plots of delays. The solid triangles (300 V/mm), squares (500 V/mm), and circles (1000 V/mm) are for ghosts from a rabbit of age 6 months. The open triangles (300 V/mm), squares (500 V/mm), and circles (1000 V/mm) are for a rabbit of age 18 months. Buffer strength, 20 mM; pulse duration, 0.9 ms; AC field strength, 8 V/mm.

1988); for example, $D = 0.55 \times 10^{-8}$ cm^2/s for the data shown in Figure 2]. This gives a value of about 0.1 s. A rigorous solution of the time-dependent diffusion equation gave an even lower value of the time for horn formation (Dimitrov, unpublished results). The estimate of this time was based on the assumption that the earliest indication of the fluorescence in the unlabeled membrane can be detected when the fluorescent dye concentration reaches 10% of the dye concentration in the originally labeled membrane.

Most of the earlier studies of electrofusion used the criterion of the microscopic observation of the formation of one large spherical cell from two or more smaller cells in contact (Zimmermann, 1982; Zimmermann et al., 1988). The time resolution of those methods was of the order of seconds to minutes. Often fusion was recognized as the rounding-up process rather than the more rigorous membrane mixing and contents mixing criteria (Sowers, 1988, 1989c; Sarkar et al., 1989; Stenger & Hui, 1989).

The lack of clear experimental data for the initial stages of membrane electrofusion and the similarity in pulse characteristics used for both electroporation and electrofusion (Zhelev et al., 1988; Melikyan & Chernomordik, 1989) led to the view that membrane merging, as one of the stages of cell fusion (Rand & Parsegian, 1986), can occur during the pulse (Zimmermann, 1982; Zhelev et al., 1988; Dimitrov & Zhelev, 1988; Stenger & Hui, 1989). In support of this view are data on electrofusion kinetics monitored by contents mixing assays (Stenger & Hui, 1989). These observations did not show any delay between the fusogenic pulse and the fluorescence increase as an indicator of cell fusion (Stenger & Hui, 1989). However, the lack of delay in their experiments may have been due to the fast electroosmotic exchange of the water-soluble probe through the pores before the fusion takes place (Sowers, 1988; Dimitrov & Sowers, 1990). Recent theoretical work seemed to support the possibility for membrane merging during the pulse (Dimitrov & Zhelev, 1988). It was also estimated that the current through the pores during the pulse gives rise to strong intermembrane attraction (Pastushenko, personal communication). The attractive force can overcome the hydration barrier and induce membrane merging during the pulse.

The discovery of a long-lived "fusogenic" state (Sowers, 1986; Teissie & Rols, 1986) showed, however, that membrane merging can take place after the pulse. Experiments with erythrocyte ghosts showed that fusion can occur even if the

membrane contact is induced many seconds after the high-voltage pulse (Sowers, 1986). The fusogenic membrane alteration was found to be local and laterally immobile (Sowers, 1987). Therefore, the pulse induces long-lived structural rearrangements in the membrane. Structural changes after high-voltage electric pulses were also recorded with NMR (Lopez et al., 1988). The conclusion is that the membrane retains its ability to fuse for a relatively long period of time after the pulse.

Mechanisms of Fusion. The discovery of the long-lived fusogenic states proves that membranes can fuse at a significant time *after* the pulse. The very short delays (<50 ms) at high-voltage pulses (Figure 3) and high temperature (Figure 9) indicate that membranes may merge *during* the pulse. The very long delays (>3 s) at low pulse field strength (Figure 3), short pulse duration (Figure 4), high medium viscosity (Figure 8), or large intermembrane separations (Figure 5) show that it may take time for membranes to merge and permit the dye to begin to laterally diffuse through the sites where fusion took place.

Another possible explanation for the long delays is that the intermembrane connections (fusion sites) which form during the pulse are very small in size and/or number. Then the delay can be the time for the dye to diffuse through these structures. While this can certainly reflect the dependence of the delay on the pulse strength and duration, it is difficult to account for the dependence on the viscosity of the medium (Figure 8) and the AC field strength (Figure 5). The increase in size of the intermembrane connections with time may depend on the medium viscosity, because it causes hydrodynamic resistance.

However, the size of the fusion sites can be large. One may expect that the initial size of the fusion intermediates will be proportional to the size of the electropores. The electropore diameter for erythrocyte ghosts is at least 5 nm (Dimitrov & Sowers, 1990). Pores with diameters between 25 and 110 nm were found with densities up to 7 μm^{-2} in erythrocyte membranes within 3 ms after pulse application (Chang & Reese, 1990). Other observations revealed areas with diameters of the order of 100 nm where the aqueous boundary between the two erythrocyte membranes is not readily distinguished within 100 ms after the pulse (Stenger & Hui, 1989). It can be theoretically estimated that if a fusion site forms and has a diameter of 10 nm or more and the diffusion coefficient of the dye in the channel is the same as for the membrane, long delays might not be expected (Dimitrov, unpublished results). Therefore, the viscosity dependence of the delay (Figure 8) may indicate the need for a certain period of time for approach of opposite fusogenic sites to reach molecular contact. This view is consistent with previous theoretical estimates (Dimitrov, 1983; Dimitrov & Jain, 1984).

The decrease in the delay which occurs with an increase of the AC field strength (Figure 5) may be due to a combination of (1) the decreased intermembrane separation that would be expected with a higher force during dielectrophoresis and (2) a larger mutual contact area (Dimitrov et al., 1990).

The presence of hemoglobin inside the ghosts does not significantly affect the delay (Figure 6), but it does increase the fusion yield and in a way which indicates that it is not due to osmotic pressure (Sowers, 1990). Therefore, the delay and fusion yield are two observable components of a fusion event which can be separated from one another by changes in hemoglobin concentration.

When the fusogenic pulse has a low electric field strength, the delay is not affected significantly, while the fusion yield changes drastically (see fusion yield increase from 20 to 74% and delay decrease from 4 to 3 s for a change in fusogenic pulse strength from 250 to 300 V/mm in Table II). The opposite is true for strong fusogens (e.g., all fusogenic pulse strengths above 350 V/mm in Table II)—the fusion yield is near saturation while the delay changes significantly. This is further evidence that the delay is a component of a fusion event which is separable from the component which controls fusion yield.

The fusion yield and the delay are similar with respect to the dependence on pulses of different duration and strength. The reciprocity between the pulse strength and duration in both electroporation and electrofusion has been well documented (Zimmermann, 1982; Zhelev et al., 1988; Sowers, 1989c; Melikyan & Chernomordik, 1989). Fusion yield, for example, can be the same for pulses of high strength and short duration as for pulses of low voltage and long duration (Sowers, 1989c). Figure 4 shows that this is also valid for the delay.

Membrane Fluidity and Fusion Kinetics. The temperature dependence of the delay (Figure 9) may be based on changes in membrane fluidity. The measured lateral diffusion coefficients [our data and data of Wu et al. (1977), Bloom and Webb (1983) and Sowers (1988)] decrease 2–3 times with an increase of temperature of 15 °C. The activation energy for the delay is 17 kcal/mol, which is the same order of magnitude as for lateral diffusion (Bloom & Webb, 1983).

It is important that the activation energy is independent of the fusogen pulse strength. This may show that the molecular rearrangements following the molecular contact and leading to membrane continuity are essentially the same for pulses of different strength. The rate of these changes should depend strongly on the membrane fluidity and not so significantly on the pulse strength.

Do the Membranes Merge during the Pulse or after the Pulse? The shortest delays we obtained (17–30 ms) are so close to the lifetime of the fusogenic pulse (8–12 ms) and the time resolution of the detection system (17 ms) that it is possible that the membranes fused during the pulse. The delays do not exist when the pulse strength is high and its duration is long, the membranes are at very close apposition, the medium viscosity is low, and the temperature is high. However, it may take time for membrane approach and molecular rearrangements after the pulse before the actual membrane fusion occurs when the experimental conditions do not strongly favor fusion. Therefore, when the delay is below the diffusion time for horn formation (<100 ms), one can expect membrane merging during the pulse; otherwise, the membranes coalesce after the pulse.

Similarity between Viral Fusion and Electrofusion. That the fusion of some viruses resembles electrofusion is supported by at least three observations: (1) Once influenza hemagglutinin is activated by low pH, fusion proceeds even if the preparation is returned to the preactivation pH (Morris et al., 1989). In electrofusion the "activation" role is played by the electric pulse. (2) The activation energy for viral fusion (in the range of 15–30 kcal/mol) is of the same order of magnitude as for electrofusion. (3) The functional dependence of the delay in the fusion of vesicular stomatitis viruses with erythrocyte ghosts on hydrogen ion concentration (Clague et al., 1990) qualitatively resembles the dependence of the delay on the pulse strength (Figures 3 and 9A) in electrofusion of erythrocyte ghosts if the pulse strength is substituted for the hydrogen ion concentration.

These common features of viral fusion and electrofusion indicate that the underlying mechanisms may be similar. In both cases the trigger of fusion (electric pulse or pH) can induce relatively long-lived fusogenic states. The nature of

these states in the case of viral fusion is related to conformational changes of the fusion protein, which exposes hydrophobic surfaces. The fusogenic states in electrofusion are commonly related to opening of pores and may involve proteins. The similarity between viral and electric field induced fusion may indicate that fusogenic states in electrofusion may involve protein-based local increases in hydrophobicity and charge redistribution. If this is so, electrofusion can become a tool for investigating mechanisms of viral fusion with the advantages of a fast and easily controlled fusogen.

Conclusions. This paper presents the first observations of the existence of a delay between the application of a fusogenic pulse and the earliest indication of fusion. This delay may reflect the lifetime of a long-lived intermediate state in membrane fusion or a prefusion membrane change leading to fusion. Either the intermediate state is two separate membranes in a fusogenic state, which approach locally each other to make molecular contact after the pulse, or it is membranes merging during the pulse.

ACKNOWLEDGMENTS

The expert technical assistance of Ms. Myoung Soon Cho is gratefully acknowledged. We thank Ms. M. Apostolova for data processing.

REFERENCES

Bloom, J. A., & Webb, W. W. (1983) *Biophys. J. 42*, 295–305.
Chang, D. C., & Reese, T. S. (1990) *Biophys. J. 55*, 1–12.
Chernomordik, L. V., Melikyan, G. B., & Chizmadzhev, Yu. A. (1987) *Biochim. Biophys. Acta 906*, 309–352.
Clague, M. J., Schoch, C., Zech, L., & Blumenthal, R. (1990) *Biochemistry 29*, 1303–1308.
Cohen, F. S., Akabas, M. H., Zimmerberg, J., & Finkelstein, A. (1984) *J. Cell Biol. 98*, 1054–1062.
Cohen, F. S., Niles, W. D., & Akabas, M. H. (1989) *J. Gen. Physiol. 93*, 201–210.
Dimitrov, D. S. (1983) *Prog. Surf. Sci. 14*, 295–424.
Dimitrov, D. S., & Jain, R. K. (1984) *Biochim. Biophys. Acta 779*, 437–468.
Dimitrov, D. S., & Zhelev, D. V. (1988) *Colloid Polym. Sci. 76*, 26–31.
Dimitrov, D. S., & Sowers, A. E. (1990) *Biochim. Biophys. Acta 1022*, 381–392.
Dimitrov, D. S., Apostolova, M. A., & Sowers, A. E. (1990) *Biochim. Biophys. Acta 1023*, 389–397.
Dodge, J. T., Mitchell, C., & Hanahan, D. J. (1963) *Arch. Biochem. Biophys. 100*, 119–130.
Duzgunes, N., Allen, T. M., Fedor, J., & Papahadjopoulos, D. (1987) *Biochemistry 26*, 8435–8442.
Georgiou, G. N., Morrison, I. E. G., & Cherry, R. J. (1989) *FEBS Lett. 250*, 487–492.
Heuser, J. E., Reese, T. S., Dennis, M. J., Jan, Y., Jan, L., & Evans, L. (1979) *J. Cell Biol. 81*, 275–300.
Hoekstra, D., & Wilschut, J. (1989) in *Water Transport in Biological Membranes* (Benga, G., Ed.) Vol. 1, From Model Membranes to Isolated Cells, pp 143–176, CRC Press, Boca Raton, FL.
Hoekstra, D., Duzgunes, N., & Wilschut, J. (1985) *Biochemistry 24*, 565–572.
Hoekstra, D., Klappe, K., Hoff, H., & Nir, S. (1989) *J. Biol. Chem. 264*, 6786–6792.
Laggner, P. (1988) *Top. Curr. Chem. 145*, 173–202.
Lopez, A., Rols, M. P., & Teissie, J. (1988) *Biochemistry 27*, 1222–1228.
Meers, P., Hong, K., & Papahadjopoulos, D. (1988) *Biochemistry 27*, 6784–6794.
Melikyan, G. B., & Chernomordik, L. V. (1989) in *Electroporation and Electrofusion in Cell Biology* (Neumann, E., Sowers, A. E., & Jordan, C. A., Eds.) pp 181–192, Plenum Press, New York.
Morris, S. J., Sarkar, D. P., White, J. M., & Blumenthal, R. (1989) *J. Biol. Chem. 264*, 3972–3978.
Niles, W. D., & Cohen, F. S. (1987) *J. Gen. Physiol. 90*, 703–735.
Plattner, H. (1989) *Int. Rev. Cytol. 119*, 197–286.
Pohl, H. A. (1978) *Dielectrophoresis*, Cambridge University Press, London.
Rand, R. P., & Parsegian, V. A. (1986) *Annu. Rev. Physiol. 48*, 201–212.
Rupert, L. A. M., Engberts, J. B. F. N., & Hoekstra, D. (1988) *Biochemistry 27*, 8232–8239.
Sarkar, D. P., Morris, S. J., Eidelman, O., Zimmerberg, J., & Blumenthal, R. (1989) *J. Cell Biol. 109*, 113–122.
Siegel, D. P. (1984) *Biophys. J. 45*, 399–420.
Siegel, D. P. (1986) *Biophys. J. 49*, 1171–1183.
Siegel, D. P., Banschbach, J., & Yeagle, P. L. (1989) *Biochemistry 28*, 5010–5019.
Sowers, A. E. (1984) *J. Cell Biol. 99*, 1989–1996.
Sowers, A. E. (1986) *J. Cell Biol. 102*, 1358–1362.
Sowers, A. E. (1987) *Cell Fusion*, Plenum Press, New York.
Sowers, A. E. (1988) *Biophys. J. 54*, 619–626.
Sowers, A. E. (1989a) *Biochim. Biophys. Acta 985*, 334–338.
Sowers, A. E. (1989b) *Biochim. Biophys. Acta 985*, 339–342.
Sowers, A. E. (1989c) in *Electroporation and Electrofusion in Cell Biology* (Neumann, E., Sowers, A. E., & Jordan, C. A., Eds.) pp 229–256, Plenum Press, New York.
Sowers, A. E. (1990) *Biochim. Biophys. Acta 1025*, 247–251.
Spruce, A. E., Iwata, A., White, J. M., & Almers, W. (1989) *Nature 342*, 555–558.
Stenger, D. A., & Hui, S. W. (1989) in *Electroporation and Electrofusion in Cell Biology* (Neumann, E., Sowers, A. E., & Jordan, C. A., Eds.) pp 167–180, Plenum Press, New York.
Teissie, I., & Rols, M. P. (1986) *Biochem. Biophys. Res. Commun. 140*, 258–266.
Weast, R. C. (1989) *Handbook of Chemistry and Physics*, CRC Press, Boca Raton, FL.
Woodbury, D. J., & Hall, J. E. (1988a) *Biophys. J. 54*, 1053–1063.
Woodbury, D. J., & Hall, J. E. (1988b) *Biophys. J. 54*, 345–349.
Wu, E., Jacobson, K., & Papahadjopoulos, D. (1977) *Biochemistry 16*, 3936–3941.
Zhelev, D. V., Dimitrov, D. S., & Doinov, P. (1988) *Bioelectrochem. Bioenerg. 20*, 155–167.
Zimmermann, U. (1982) *Biochim. Biophys. Acta 694*, 227–277.
Zimmermann, U., Arnold, W. M., & Mehrle, W. (1988) *J. Electrost. 21*, 309–345.